

We are IntechOpen, the world's leading publisher of Open Access books Built by scientists, for scientists

6,900

Open access books available

186,000

International authors and editors

200M

Downloads

Our authors are among the

154

Countries delivered to

TOP 1%

most cited scientists

12.2%

Contributors from top 500 universities



WEB OF SCIENCE™

Selection of our books indexed in the Book Citation Index
in Web of Science™ Core Collection (BKCI)

Interested in publishing with us?
Contact book.department@intechopen.com

Numbers displayed above are based on latest data collected.
For more information visit www.intechopen.com



Real-Time Implementation of the Advanced Control of the Three-Phase Induction Machine Based on Power Inverters

Marian Gaiceanu

Additional information is available at the end of the chapter

<http://dx.doi.org/10.5772/intechopen.68217>

Abstract

The fast growing development of both the numerical equipment and power electronics allows the rapid prototyping of the innovating idea. The objective of this chapter is to put into evidence the teaching aspects through the applicative research in the field of the electric drives. The chapter provides the basic and advanced aspects of the electric drives control based on the most used electrical machine: three-phase induction motor (IM). The research work is presented in didactical way, starting with the conventional vector control, followed by the integration of the model reference adaptive control into the specific IM-based drive. The verified numerical simulation results push the research process through the implementation way. In order to increase the IM drives efficiency, the real-time implementation of the most commonly used modulation techniques is provided. Based on the dSpace platform, interfaced by ControlDesk, the experimental results are obtained. Both the performances of the cascaded control and model reference adaptive control are shown.

Keywords: DS1104, Matlab®, Simulink, PWM, THPWM, OHPWM, power inverter, efficiency, sustainability

1. Introduction

The technical literature subject to teaching of the adjustable AC drives, at the undergraduate and post-graduate levels, offers various techniques of learning based on the computer tools [1–5]. The fast growing of the digital technology conducts to the inherent replacement of the analog control by the numerical ones. A successful AC drive-based teaching tool should include at

least the parameter identification/estimation task, the adequate control, and one friendly interface between the student and the computer. One of the first approaches of including the computer as an interactive learning environment and real-time implementation in adjustable drive teaching process is presented in Refs. [1, 2]. The virtual education environment allows the hands-on exercises to be tested and solved in a real-time environment [1, 2].

By using the obtained values from the no-load and short-circuit tests and the Matlab/Simulink software facilities [3], the electrical and mechanical parameters of the three-phase induction motor are determined. In order to teach and well understand the complex electromechanical phenomena of an adjustable speed drive based on the IM, the authors [4] use the Matlab/Simulink software as a teaching tool. The teaching tool based on the intelligent control is presented by the authors of the chapter [5]. The fuzzy logic is one of the controlled ways in order to avoid the parameter identification/estimation task of the AC drive. The modern electric drives include the increase of the efficiency in the control design process. Despite the above presented state of the art, the author of this chapter provides an original robust model reference adaptive control of the three-phase induction motor in which the parameters of the controller are provided on-line; the parameters being adapted through the on-line estimator.

A major key-enabled technology for sustainability of the electrical energy is the enhancement of the efficiency characteristics in power inverter applications. Therefore, both energy saving potential and optimization of the energy consumption should be explored [6]. For the electric drives area, combining variable speed drives with modulation techniques could be one way of sustainability of both the electrical energy producers and consumers. Another way of assuring the sustainability of the electric drives is the use of the optimal control theory [6]. The power electronics is other key enabling technology in energy efficiency, as well in production, distribution and energy transport [5]. This chapter provides solutions both to increase the power quality and efficiency of the static power inverter. The chapter offers, in the didactical manner, the basic theoretical concerns regarding the static conversion by means of the power inverters, mathematical modelling of the power inverter, the modulation strategies, the numerical simulation and the experimental results for the presented modulation techniques. The chapter is addressed to the future and current changeable actors: the students, researchers and engineers. The chapter contains the basic concepts and techniques to design, simulate and implement the efficient power inverters through a Matlab-Simulink well-structured technical guide. In this manner, the chapter is addressed both to the students and researchers in the field of the electric drives. The mathematical model of the power inverter combined with the rotor field vector control of the three-phase induction machine (IM) is provided in Section 2. In Section 3, an overview of the modulation techniques is given with the purpose to point out the development trend in the power inverters technology. Moreover, the original model reference adaptive control of the three-phase induction machine is provided in Section 4.

2. Field-oriented control of the three-phase induction machine

In industry, the most commonly used electric drive is based on the three-phase induction machine (IM). It is well known that the mathematical model of the three-phase induction

machine is nonlinear (the nonlinearities type are product, saturation and hysteresis), being a multivariable coupling of the control structure. For the same size, weight and inertia, the performances of the IM are higher than that of the DC motor. Therefore, the efficiency and the maximum speed are superior to that of the DC motor, in the lower price. From the electrical drive point of view, there are mainly two types of control: scalar and vectorial. At the constant flux, due to the decoupling control, the performances of the vector-control IM drives are better than of the scalar drives.

The field-oriented control concept allows independent control of the mechanical and electrical circuits through the stator active and reactive components. The field-oriented control could be in direct form or indirect form, depending on the flux vector position determination. The invariance propriety of the electromagnetic torque to the reference frames conduct to the three basic field-oriented schemes: stator field-oriented control, rotor field-oriented control, air-gap or arbitrary field-oriented control. The most used one is the rotor-magnetizing current reference frame [6] that rotates synchronously with the angular speed of the rotor-magnetizing current phasor. In order to apply this type of the vector control, the phasor of the rotor-magnetizing current should be known. This requirement assumes the real-time calculus of the position and the modulus of the magnetizing current phasor.

Due to the orthogonality between the stator and rotor magnetic fields, by neglecting the saturation, the magnetic flux depends on the stator current, without being influenced by the rotor current. By aligning the rotor-magnetizing phasor with the d axis of the synchronously (d, q) quadrature reference frame, the components of it are as follows:

$$\lambda_{qr} = 0, \lambda_{dr} = \lambda_r = \lambda = ct. \quad (1)$$

In rotor field reference frame, the mathematical model of the three-phase induction machine is as follows [6, 7]:

$$\begin{aligned} \sigma T_s \frac{di_{ds}}{dt} + i_{ds} &= \frac{v_{ds}}{R_s} - (1 - \sigma) T_s \frac{di_{mR}}{dt} + \sigma T_s \omega_{mR} i_{qs} \\ \sigma T_s \frac{di_{qs}}{dt} + i_{qs} &= \frac{v_{qs}}{R_s} - (1 - \sigma) T_s \omega_{mR} i_{mR} - \sigma T_s \omega_{mR} i_{ds} \\ T_r \frac{di_{mR}}{dt} + i_{mR} &= i_{ds} \\ J \frac{d\omega_r}{dt} &= k_T i_{mR} i_{qs} - T_L \\ \omega_{mR} &= \omega_r + \omega_{sl}, \quad \omega_{sl} = \frac{R_r}{L_m} \frac{i_{qs}}{i_{mR}} \end{aligned} \quad (2)$$

By taking into account the above mentioned system equations (2), the coupling between the d and q voltage components could be noticed. By adding the adequate feedforward electromotive voltage components, E_d and E_q , the IM mathematical model could be decoupled (**Figure 1**) [6, 7]:

In order to supply adequate power to the IM, the three-phase power inverter is necessary. By comparing the v_{ds}^* (v_{qs}^*) d -axis stator reference voltage and q -axis stator reference voltage with the carrier signal, the adequate switching states are delivered. This task is accomplished by the modulators.

In **Figure 2**, the Simulink implementation of the rotor field vector control of the three-phase induction machine is shown.

The Proportional-Integral (PI) speed and flux controllers are shown in **Figure 3**.

In **Figure 4**, the rotor magnetic flux position is shown [8]. In the Simulink group shown in **Figure 5**, the PI d - q current controllers and voltage decoupling terms are added.

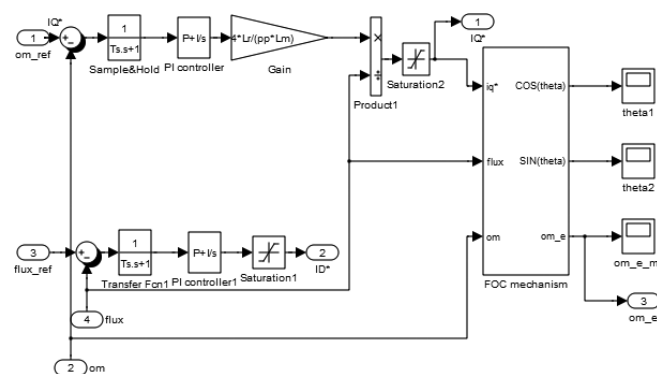


Figure 3. The control side of the FOC with IM.

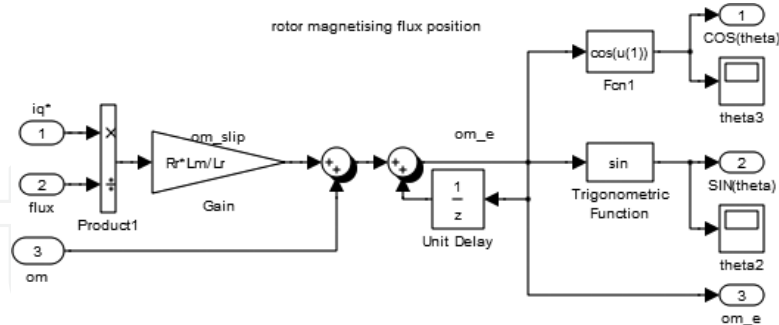


Figure 4. Determination of the synchronous reference frame position.

In **Figure 6**, both the inverter transfer function and the stator equivalent d - q windings are shown.

By using the Simulink program described in this chapter, the references and the output state variables are presented in **Figure 7**. The inner torque control loop is tuned by using the modulus criterion. The speed outer loop control is performed based on the symmetrical

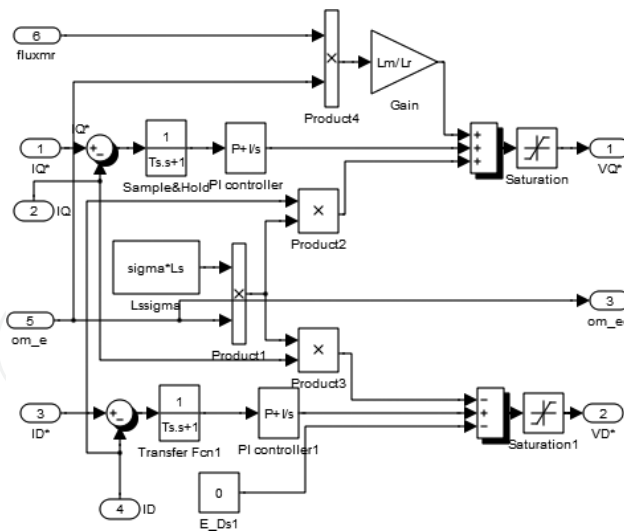


Figure 5. Current control and the voltage decoupling block.

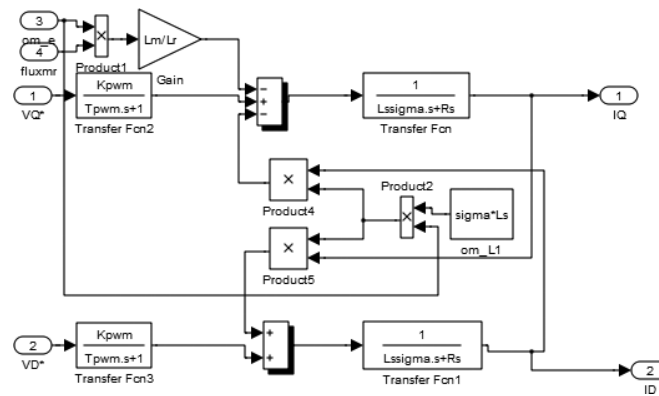


Figure 6. The power inverter transfer function and the equivalent stator windings of the three-phase IM.

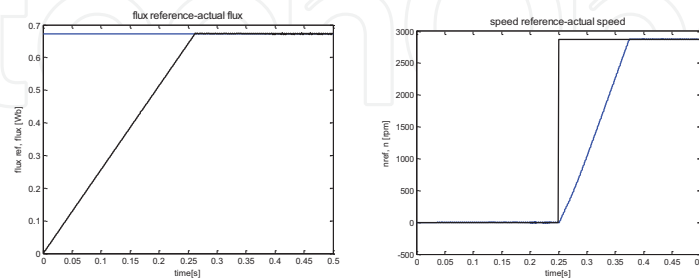


Figure 7. The comparison between the input and output signals of the FOC with IM drive.

criterion. Based on the nameplate motor data presented in **Table 1**, the Matlab script providing automatically the parameters of the tuned speed and current controllers is depicted in Ref. [8].

Parameters	Value	Parameters	Value	Parameters	Value
Rated power	$P_n=45$ kW	Power factor	0.86	Rated flux	0.67 Wb
Rated speed	2980 rpm	Rated efficiency	0.92	J	0.15 kgm ²
R.m.s line voltage	380 V	R_s	0.0763Ω	I_{mN}	18.86 A
Rated frequency	50Hz	R_r	0.0261Ω	Rated load torque	144 Nm
Rated current	87 A	L_{sc}	0.0009 H		

Table 1. The nameplate data of the three-phase induction motor.

3. The modulation techniques

In order to increase both the efficiency and the harmonic contents of the three-phase power inverter, four types of modulation strategies have been implemented in real time using dSpace platform. The implemented modulation strategies [9–12] are as follows: (1) sinusoidal modulation— Sinusoidal Pulse Width Modulation (SPWM), (2) Third harmonic insertion—Third harmonic Pulse Width Modulation (THPWM), (3) space vector modulation—space vector Pulse Width Modulation (SVPWM) and (4) optimized modulation—optimized modulation Pulse Width Modulation (OPWM). The first approach is the *rectangular pulse modulation*. This method raises harmonic distortion problems, and the amplitude of the fundamental component of the output voltage is fixed. However, the frequency could be varied. In order to obtain adjustable amplitude, a derivative method has been deducted: the *quasi-rectangular pulse modulation*. Nowadays, the most used method is the *Sinusoidal Pulse Width Modulation* (SPWM) due to the introduction of three degrees of freedom—the phase, the frequency and the amplitude of the fundamental component of the alternative output voltage. Additionally, the harmonics content of the output signal is considerably diminished. Another issue of the static power inverters is the DC link voltage utilization. By means of the modulation techniques significant improvement of the power inverter efficiency and harmonics content of the output signals could be obtained. The most common modulation technique is the sinusoidal pulse width modulation (SPWM). The SPWM method introduces an important advantage: generates the high order harmonics, therefore the lower weight of the filter inductance is obtained in order to compensate them.

In **Figure 8**, the three-phase power inverter schematic is shown ($v_{s1,n}$, the voltage between the 1 and n potentials; V_{dc} the DC link voltage).

Based on the analysis of the control signal and the carrier signal, by deducting the conduction time, t_{on} , the analytic formula of the SPWM duty cycle is deducted as follows:

$$d_1 = \left\lfloor \frac{1}{2} \right\rfloor + \frac{1}{2} \left(\frac{v_{s1,n}}{V_{dc}/2} \right) \quad (5)$$

The modulator has been implemented in real time through the dSpace platform (**Figure 9**):

By using the implemented cascade control (**Figure 2**) in the dSpace platform, the speed reference has been followed and the following three-phase inverter output currents have been obtained (**Figure 10**).

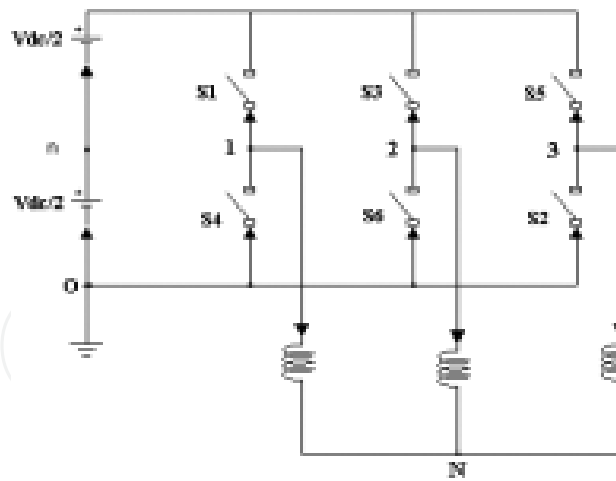


Figure 8. Three-phase power inverter schematic.

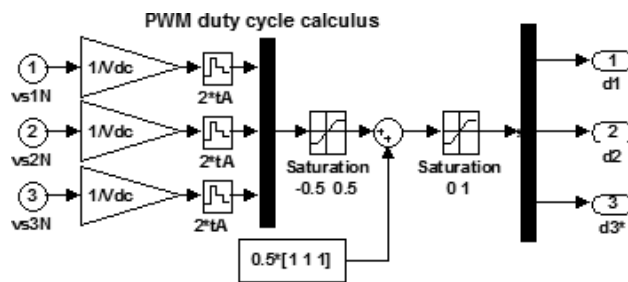


Figure 9. Matlab-Simulink implementation of the sinusoidal PWM modulation technique.

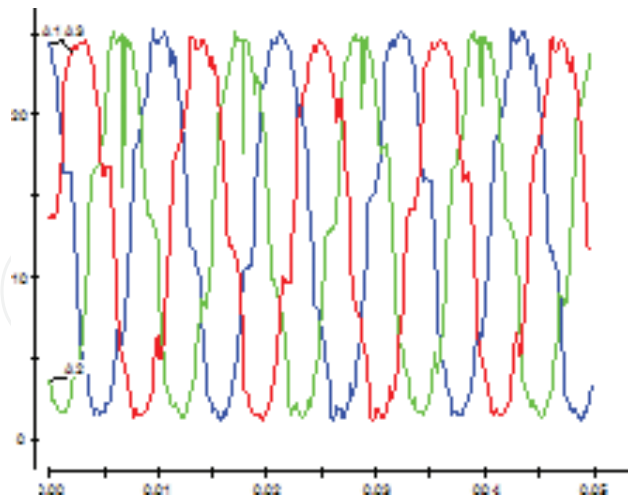


Figure 10. The output currents of the three-phase power inverter with sinusoidal modulation.

The real-time implementation results of the speed control are shown in **Figures 11** and **12**. The speed is reduced through the speed reference. In **Figure 11**, the performances of the speed control are shown (The step signal is the speed reference and the delayed one is the feedback speed).

By using the adequate modulation techniques, the efficiency of the power conversion could be increased.

By inserting the *third harmonic component* in the sinusoidal waveform (**Figure 13**), the three-phase reference voltages are obtained (**Figure 14a**). The improved efficiency and the decreased harmonic content will be obtained by means of the *space vector modulation technique* (**Figure 14b**). In order to minimize the number of the switching, the *optimized modulation technique* could be applied (**Figure 14c**).

The optimized modulation could be applied for the isolated three-phase load as IM. The optimized modulation (**Figure 14c**) minimizes the number of commutations by subtracting a

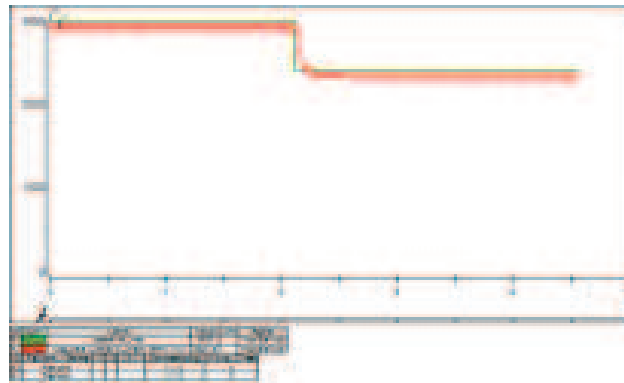


Figure 11. The real-time speed control of the IM based on the dSpace platform.

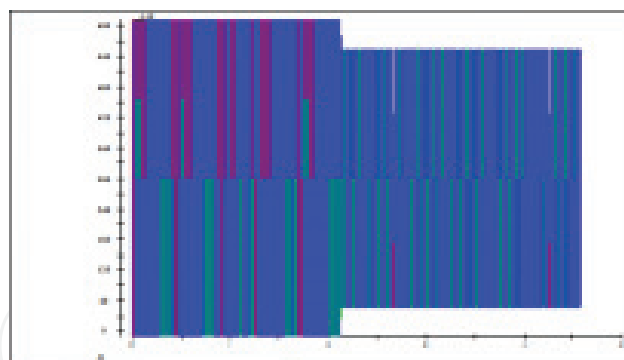


Figure 12. The corresponding three-phase power inverter output voltages.

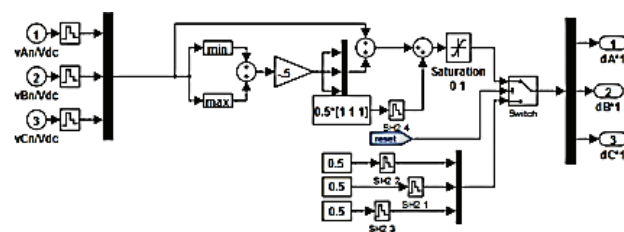


Figure 13. The Simulink implementation of the *third harmonic component* insertion and of the sinusoidal PWM.

zero sequence signal, u_z^* [Eq. (6)], from the sinusoidal voltages [Eq. (7)]. In this way, the usage of the DC link voltage is increased. In **Figure 15**, the dSpace implementation of the OPWM is shown.

$$u_z^* = -\min\left[\frac{U_{dc}}{2} - \max(u_a^*, u_b^*, u_c^*), \frac{U_{dc}}{2} - \min(u_a^*, u_b^*, u_c^*)\right] \quad (6)$$

$$\begin{aligned} u_a^{**}(t) &= u_a^*(t) - u_z^*(t) \\ u_b^{**}(t) &= u_b^*(t) - u_z^*(t) \\ u_c^{**}(t) &= u_c^*(t) - u_z^*(t) \end{aligned} \quad (7)$$

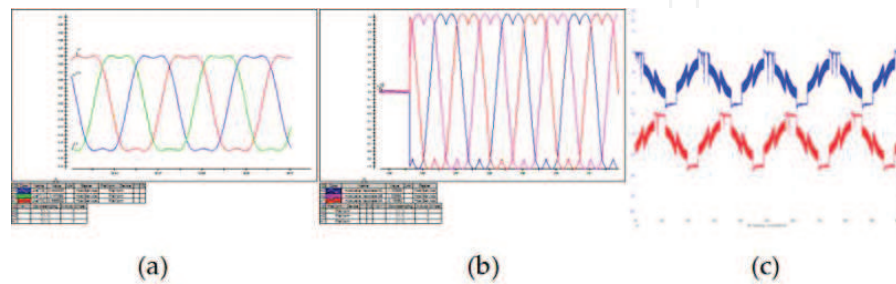


Figure 14. The reference signals for different modulation techniques (a) the TH-PWM, (b) space vector SV-PWM and (c) optimized modulation (O-PWM).

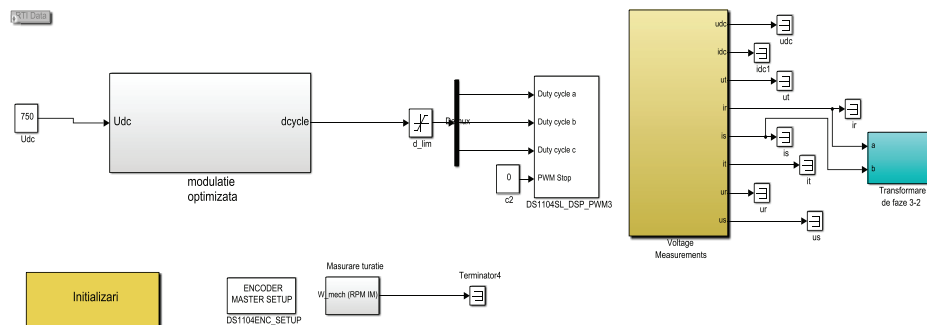


Figure 15. Block diagram of the dSpace implementation of the optimized modulation.

4. The advanced control of the three-phase induction machine based on power inverter

In this section, the advanced control of the IM drive is provided taken into consideration the on-line estimation of the controller parameters. Therefore, the variation of the parameters does not affect the controller performances. The presented adaptive control is robust to unmodelled parameter variations and structural uncertainty. The model reference adaptive control, in direct form, unnormalized of the three-phase induction machine has been used (**Figure 16**)

[13, 14]. The adaptive control $u(t)$ contains two components: the gradient ($\theta_g \in \mathcal{R}^{2n}$) and the variable structure ($\theta_v \in \mathcal{R}^{2n}$):

$$u(t) = \theta^T(t)v(t), \theta = \theta_g + \theta_v \quad (8)$$

In **Figure 17**, the Simulink implementation of the rotor field-oriented control of the IM (supposing the constant magnetizing current at the rated value) is shown.

In order to obtain the adaptive control (8), the vector of the filtered signals should be known:

$$v(t) = [v_u^T(t) \quad v_y^T(t) \quad y_p(t) \quad r(t)]^T \in \mathcal{R}^{2n_p}, \quad (9)$$

where $r(t)$ is the reference of the adaptive system; $y_p(t)$ the output signal of the process; $v_u \in \mathcal{R}^{n_p-1}$ the dynamic of the filter connected at the control, $v_y \in \mathcal{R}^{n_p-1}$ is the dynamic of the filter connected at the output of the plant [14]

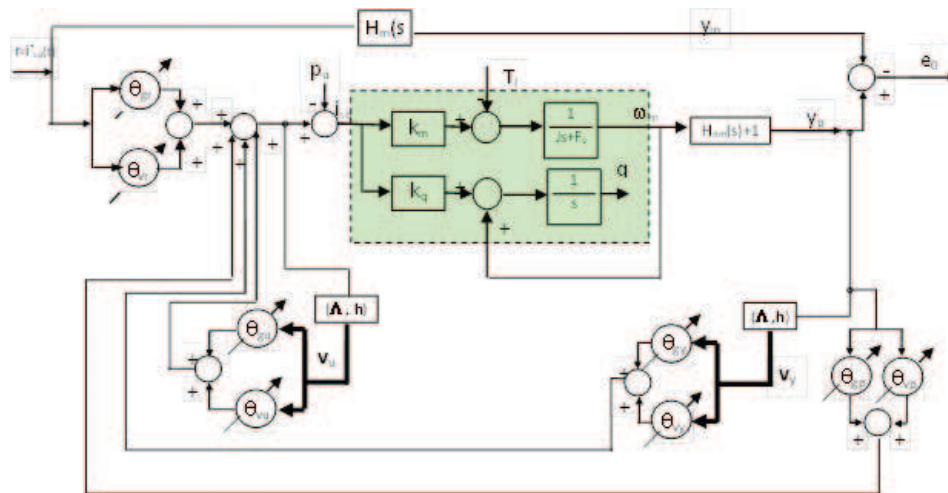


Figure 16. The block diagram of the three-phase IM model reference adaptive control.

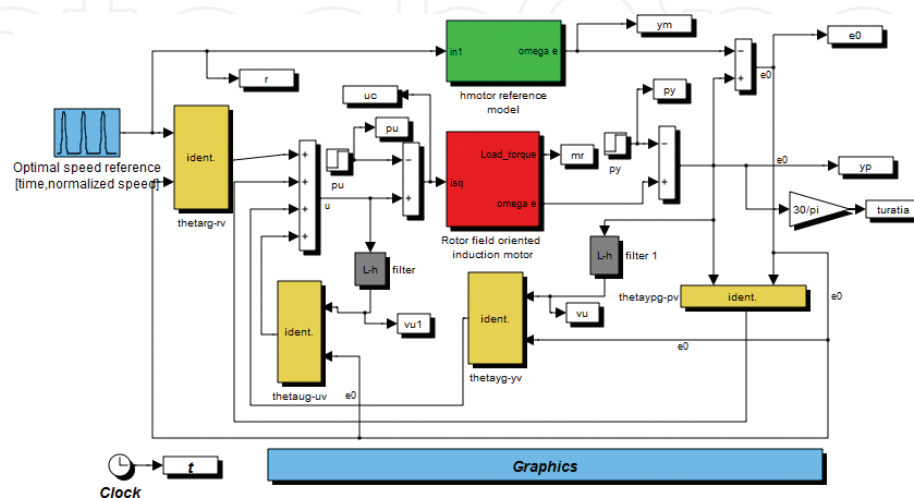


Figure 17. Simulink implementation of the model reference adaptive control with unity relative degree.

$$\begin{cases} \dot{\mathbf{v}}_u = \Lambda \mathbf{v}_u + \mathbf{h}u \\ \dot{\mathbf{v}}_y = \Lambda \mathbf{v}_y + \mathbf{h}y_p \end{cases} \quad (10)$$

where

$$\begin{aligned} v_u(s) &= (s\mathbf{I} - \Lambda)^{-1} \mathbf{h}U(s) \\ v_y(s) &= (s\mathbf{I} - \Lambda)^{-1} \mathbf{h}Y_p(s) \end{aligned} \quad (11)$$

The adaptive control is formed by two components (**Figure 18**): gradient and variable structure. The specific parameters of the above-mentioned components are calculated via **Figure 18**.

The parameters vector with gradient-adjustment control [14, 15]:

$$\theta_g \in \mathcal{R}^{2n_p} = \begin{bmatrix} \theta_{gu}^T(t) & \theta_{gy_p}^T(t) & \theta_{gp}(t) & \theta_{gr}(t) \end{bmatrix}^T \quad (12)$$

The dynamics components of the gradient parameters vector are calculated as (**Figure 18**):

$$\dot{\theta}_{gu} = -\gamma_g \cdot \text{sign}(k_p) \cdot v_u \cdot e_0 \quad (13)$$

The gradient component assures stability and makes smooth transient response and zero tracking error. The asymptotic performances will be assured by gradient-adjustment component.

The variable structure control [14]

$$u_v(t) = \theta_v^T v(t), \quad (14)$$

where the parameters vector with variable structure adjustment control are as follows:

$$\theta_v(t) = \begin{bmatrix} \theta_{vu}^T(t) & \theta_{vy_p}^T(t) & \theta_{yp}(t) & \theta_r(t) \end{bmatrix}^T. \quad (15)$$

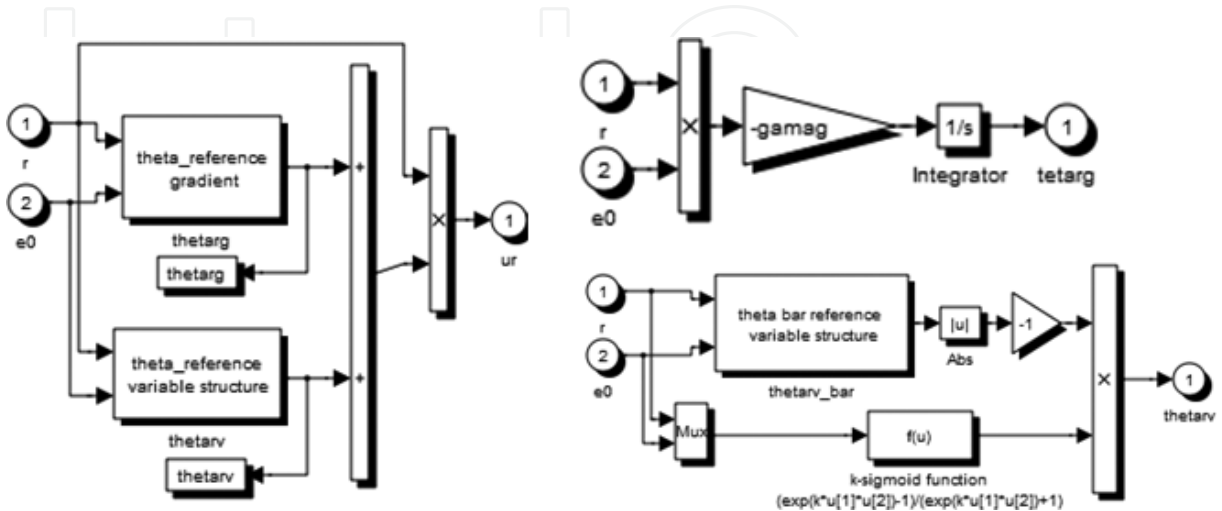


Figure 18. The gradient and variable structure components of the adaptive control. The calculation of the specific parameters (θ_g , θ_v).

The variable structure adaptive component assures a fast time response of the control by introducing a *signum* function [14]:

$$\theta_{vu} = \bar{\theta}_{vu} \text{sign}(k_p) \text{sign}(e_0 v_u). \quad (16)$$

In order to eliminate the small oscillations around the equilibrium point, the enhanced feature is included in the variable structure adaptive component [16, 17] through the *k*-sigmoid function [14, 15]:

$$\theta_{vu} \cong \bar{\theta}_{vu} \frac{e^{ke_0 v_u} - 1}{e^{ke_0 v_u} + 1} \text{sign}(k_p) \quad (17)$$

where

$$\frac{d}{dt} \bar{\theta}_{vu} = -\lambda_{vu} \bar{\theta}_{vu} - \gamma_v |e_0 v_u|. \quad (18)$$

In **Figure 19**, calculation of the parameter $\bar{\theta}_{vu}$ (mentioned in **Figure 18**) is based on Eq. (18):

In **Figure 20**, according to Eq. (10), the filtered vector calculation is shown.

In **Figure 21**, the Simulink implementation of the IM mathematical model is shown.

The differential equation of the circular motion is solved by using the Laplace transform as in **Figure 22**. The Reverse Park and Clarke transformations are implemented in Simulink [13] as in **Figures 23 and 24**. The performances of the model reference adaptive control are shown in **Figures 25–27**.

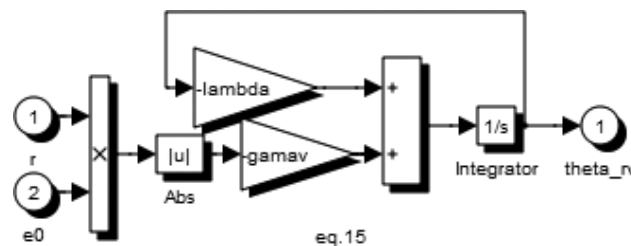


Figure 19. The parameter $\bar{\theta}_{vu}$ calculation.

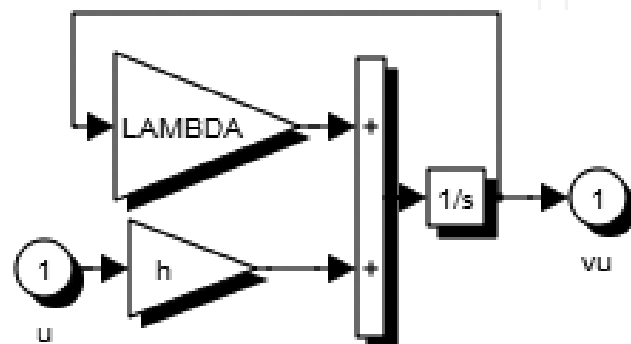


Figure 20. The filtered vector calculation.

The advanced control consists of the model reference adaptive control of three-phase induction machine. It could be noted that a robust MRAC drive system has been provided, the speed being almost insensible to load torque disturbances (Figures 25–27). Figure 25 shows the obtained adaptive control (i_{sq}) at the constant rotor-magnetizing current, the reference and the actual values of the speed references and the evolution of the tracking error. Taking into account the gradient and variable structure parameters (Figure 26), the resulted adaptive control, i_{sq} , assures the stability, robustness to load variation (Figure 27), smooth transient response of the adaptive controller parameters and zero-tracking error (Figure 26). The asymptotic performances are assured by the gradient component. In

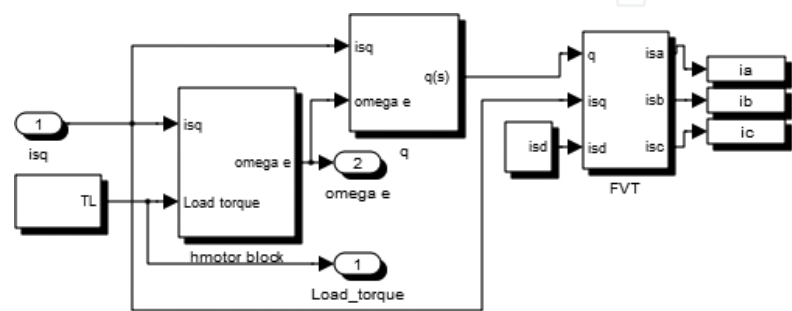


Figure 21. Simulink implementation of the IM mathematical model.

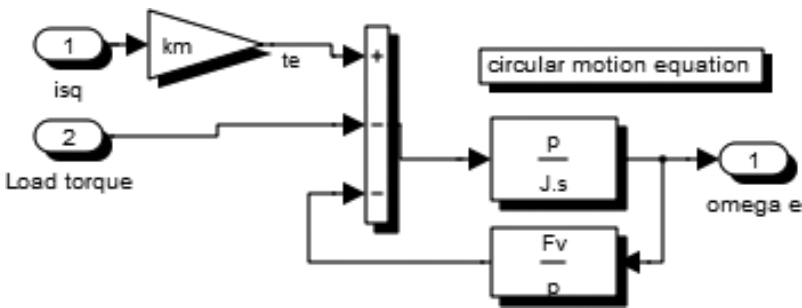


Figure 22. The solution of the mechanical equation.

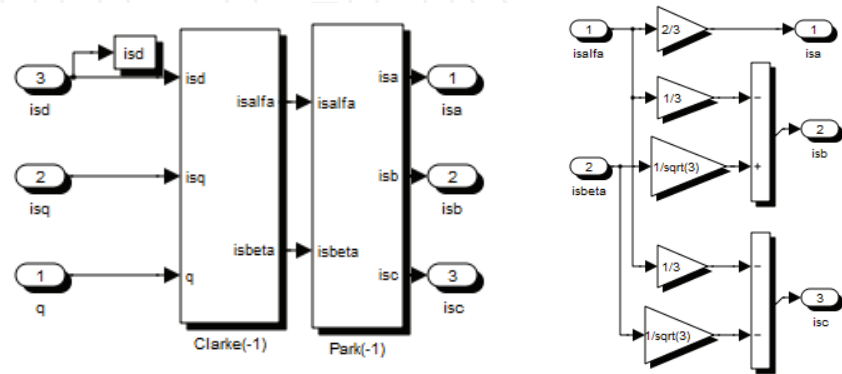


Figure 23. The Reverse Park and Clarke transformations.

Figure 27, the three-phase stator currents of the IM under the step load torque variation are shown.

In Annex I, the dSpace implementation of the stator current control of the three-phase IM with sinusoidal modulation is provided.

The first figure from the Annex I contains: (1) at the left side: the reference values of the stator frequency and the r.m.s. reference value of the stator current, the initiation of the control process (pwm_enable), the confirmation of the normal operation of the dSpace platform (dspace_ok); (2) in the middle: the control system; (3) the outputs: the duty cycles, the estimated three-phase stator voltage supply and the measured three-phase stator currents.

The second figure from the Annex I contains the measuring system of the three-phase stator currents, the stator currents references and the control system based on the proportional integral regulators. The outputs of the PI regulators are used in order to generate the sinusoidal modulation duty cycles (duty_abc).



Figure 24. The Simulink implementation of the reverse Park transformation.

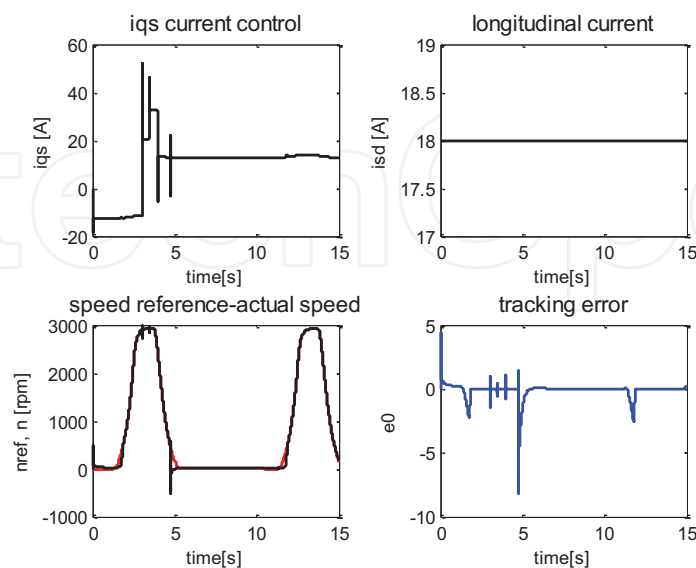


Figure 25. The adaptive control (i_{sq}) under the rated magnetization rotor flux (i_{sd}), the IM drive output (ω , angular speed) and the evolution of the tracking error (e_0).

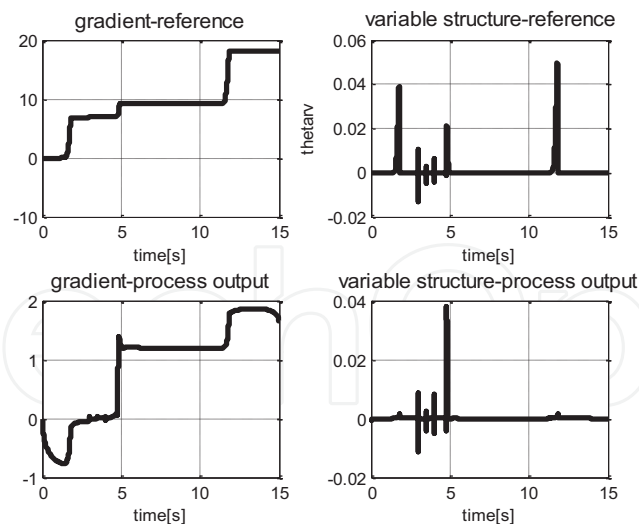


Figure 26. The evolution of the gradient and variable structure parameters.

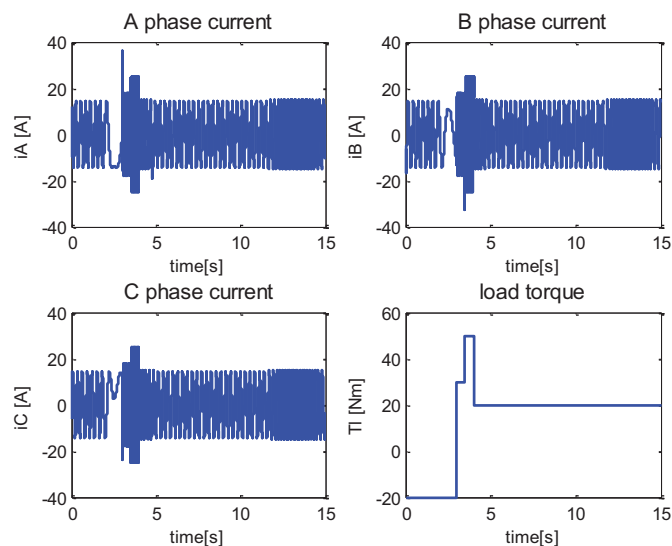


Figure 27. The three-phase stator currents under the step load torque variation.

5. Conclusions

The switching function-based mathematical modelling methodology of the full-bridge single-phase power inverter is provided. The adequate Matlab-Simulink implementation has been shown. The advantage of increasing the switching frequency by two times is taken through the unipolar asymmetric PWM modulation. Additionally, the harmonic spectrum shows a decreasing distortion in spite of the bipolar symmetric PWM modulation [8]. The chapter includes the basic theoretical aspects, followed by mathematical modelling, numerical simulations and implementation of the proposed modulation techniques capable both to increase the DC voltage usage and decrease the harmonic content of the output signals; therefore, by using Matlab/Simulink software, an efficient and clean power converter is obtained. The three-phase

power inverter connected to the three-phase induction motor is considered. The four types of the modulation techniques for the three-phase power inverter have been presented and implemented through a real-time platform: sinusoidal PWM, third harmonic insertion PWM, optimized PWM and Space Vector PWM. Moreover, the increased efficiency of the power inverter is obtained through both DC link voltage utilization and harmonic distortion reduction. In order to prove the feasibility of the provided solutions the inductive load based on the three-phase induction machine has been used supplied by means of the three-phase voltage power inverter. The SVM-PWM is considered as optimal switching modulation and due to only one transition between the two switching states excursion takes place. The flat top discontinuous PWM or optimized PWM has the advantages of minimum switching modulation and increased DC link voltage [18] is used [9]. Therefore, higher efficiency is obtained and electromagnetic compatibility is improved [10]. By inserting the third harmonic, the fundamental of the output voltage increases by 15.5% comparative with the sinusoidal PWM. The original advanced electric drive system based on the MRAC has been presented.

Acknowledgements

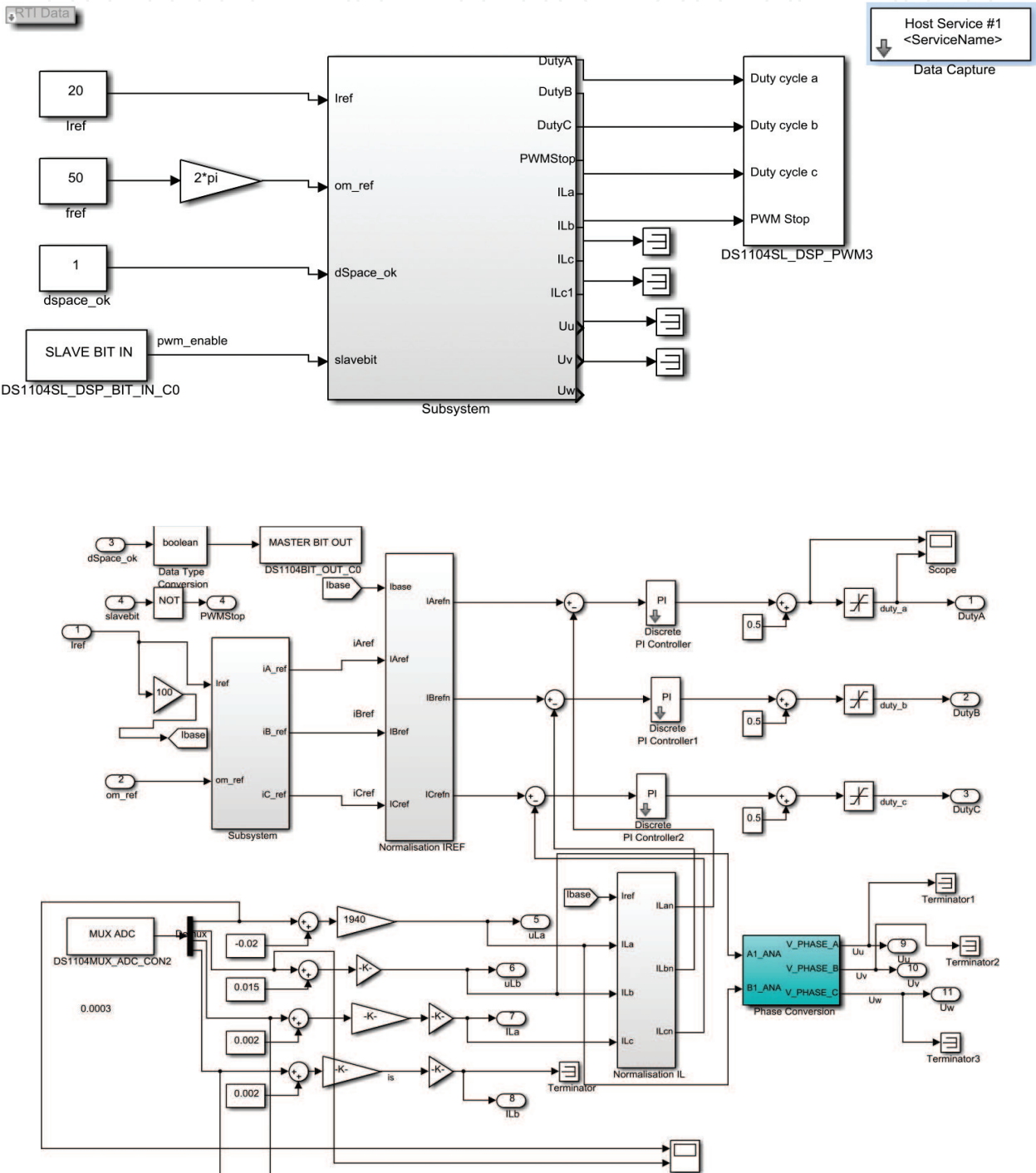
This work was supported by a grant of the Romanian National Authority for Scientific Research, CNDI-UEFISCDI, project number PN-II-PT-PCCA-2011-3.2-1680.

Nomenclature

ω_{sl}	Slip angular speed
$i_{ds} (i_{qs})$	Longitudinal stator current component d (transversal stator current component q)
$v_{ds}^* (v_{qs}^*)$	d -axis stator reference voltage (q -axis stator reference voltage)
$L_s (L_r)$	Stator inductance (rotor inductance)
L_m	Mutual inductance
$T_s=L_s/R_s$	Stator time constant
σ	Total leakage factor
T_L	The equivalent load torque reduced to the rotor shaft
$T_r=L_r/R_r$	Rotor time constant
K_T	Torque constant
J	The equivalent inertia moment
p	Number of the pole pairs
R_s, R_r	Stator and rotor phase resistance, respectively
ω_{mR}	Angular speed of the synchronous rotating frame
ω_{sl}	Slip angular frequency
ω_r	Rotor angular speed
$e_{ds}=i_{ds}^* - i_{ds}, e_{qs}=i_{qs}^* - i_{qs}$	The d - q components of the current error
i_{ds}^*, i_{qs}^*	The d - q components of the stator current references
K_p, K_i	The proportional and the integral coefficients

MRAC	Model reference adaptive control
λ_{dr}	The longitudinal (reactive) component of the rotor magnetising flux
λ_r	The rated value of the magnetic flux
λ_{qr}	The quadrature (active) component of the rotor magnetising flux

Annex I. dSpace implementation of the stator current loop control



Author details

Marian Gaiceanu

Address all correspondence to: marian.gaiceanu@ieee.org

Integrated Energy Conversion Systems and Advanced Control of Complex Processes Research Center, Dunarea de Jos University of Galati, Romania

References

- [1] Keyhani, A., Marwali, M.N., Higuera, L.E., Athalye, G., Baumgartner, G. An integrated virtual learning system for the development of motor drive systems. *IEEE Transactions on Power Systems*. 2002;**17**(1):1–6.
- [2] Mohan, N., Robbins, W.P., Imbertson, P., Undeland, T.M., Panaitescu, R.C., Jain, A.K., Begalke, T. Restructuring of first courses in power electronics and electric drives that integrates digital. *IEEE Transactions on Power Electronics*. 2003;**18**(1):429–437.
- [3] Ayasun, S., Chika, O.N. Induction motor tests using MATLAB/Simulink and their integration into undergraduate electric machinery courses. *IEEE Transactions on Education*. 2005; **48**(1): 37–46.
- [4] Saghafinia, A., Ping, H.W., Uddin, M.N., Amindoust, A. Teaching of simulation an adjustable speed drive of induction motor using MATLAB/Simulink in Advanced Electrical Machine Laboratory, 13th International Educational Technology Conference, Procedia—Social and Behavioral Sciences. 2013; **103**: 912–921. <http://www.sciencedirect.com/science/article/pii/S1877042813038585>
- [5] Elmas, C., Ali, A.M. Virtual electrical machinery laboratory: A fuzzy logic controller for induction motor drives. *International Journal on Engineering Education*. 2004; **20**(2): 226–233.
- [6] Gaiceanu, M. AC-AC Converter system for AC drives. *IEE Conference Publication Journal*.; British Library, Great Britain: Wrightsons; 2004; **2**(498):724–729. DOI: ISSN 0537-9989
- [7] Leonhard, W. *Control of Electrical Drives*. Berlin: Springer-Verlag; 1996.
- [8] Gaiceanu, M. Tool of the Complete Optimal Control for Variable Speed Electrical Drives. In: Mr Kelly Bennett, editor. *MATLAB Applications for the Practical Engineer*. InTech; Croatia, 2014; 339–374. ISBN 978-953-51-1719-3; DOI: 10.5772/57521
- [9] Kaźmierkowski, M.P., Krishnan, R., Blaabjerg, F., editors. *Control in Power Electronics: Selected Problems*. USA: Academic Press; 2002.
- [10] Analog Devices Inc. Double Update Mode of PWM Generation Unit of the ADMC401, **AN401–02**. 2000 (January).

- [11] Stumpf, P., Jordan R.K., Nagy, I. Comparison of naturally sampled PWM techniques in ultrahigh speed drives. In: International Symposium Industrial Electronics. 2012: 246–251, DOI: 10.1109/ISIE.2012.6237092 Conference: ISIE 2012, At Hangzhou, China, IEEE International Symposium on Industrial Electronics 2012, Article number 6237092, Pages 246-251, 21st. IEEE International Symposium on Industrial Electronics, ISIE 2012; Hangzhou; China; 28 May 2012 through 31 May 2012; Category number CFP12ISI-ART; Code 91747.
- [12] Rathore, A.K., Holtz, J., Boller, T. Synchronous optimal pulsewidth modulation for low-switching-frequency control of medium-voltage multilevel inverters. *IEEE Transactions on Industrial Electronics*. 2010;57(July):2374–2381.
- [13] Gaiceanu, M., Rosu, E., Dache, C., Paduraru, R., Munteanu, T. Adaptive Control of the Three-Phase Squirrel Cage Induction Motor with Load Torque Estimator. *Proceedings of the International Conference on Optimisation of Electrical and Electronic Equipment, OPTIM*. Brasov, Romania, 2012.
- [14] Filipescu, A. A compound law for adaptive and variable structure control with sigmoid function for the process with unitary relative degree model. In: *The 9th Symposium on Modelling and Identification systems; SIMSIS'94*; Galati. Romania.1994. pp. 14–18.
- [15] Ioannou, P., Fidan, B. Adaptive control tutorial. The Society for Industrial and Applied Mathematics. 2006. 2006/ xvi + 389 pages/ Softcover/ ISBN: 978-0-898716-15-3/ <http://bookstore.siam.org/dc11/>.
- [16] Orłowska-Kowalska T., Korzonek M. Stability analysis of MRASCC speed estimator in motoring and regenerating mode. *Power Electronics and Drives 2016* | Vol. 1 (36), No. 2 | pp.113–131.
- [17] Kumar, R., Das, S., Syam, P., Chattopadhyay, A.K. Review on model reference adaptive system for sensorless vector control of induction motor drives. *IET Electric Power Applications*. 2015;9(7):496–511.
- [18] Balogh, A., Varga, E., Varjasi I. DC link floating for grid connected PV converters. *World Academy of Science, Engineering and Technology, International Journal of Electrical, Computer, Energetic, Electronic and Communication Engineering*. 2008;2(4):629–634.